M^+(12-crown-4) Supramolecular Cations ($M^+ = Na^+$, K^+, Rb^+, and NH_4^+) within Ni(2-thioxo-1,3-dithiole-4,5-dithiolate)$_2$ Molecular Conductor

Tomoyuki Akutagawa,*,†,‡ Tatsuo Hasegawa,† Takayoshi Nakamura,*,† Sadamu Takeda,§ Tamotsu Inabe,|| Ken-ichi Sugiura,⊥ Yoshiteru Sakata,⊥ and Allan E. Underhill#

Research Institute for Electronic Science, Hokkaido University, Sapporo 060-0812, Japan, PRESTO, Japan Science and Technology Corporation, Japan, Department of Engineering, Gunma University, Kiryu, Gunma 376-8515, Japan, Graduate School of Science, Hokkaido University, Sapporo 060-0810, Japan, Institute of Scientific and Industrial Research, Osaka University, Ibaraki, Osaka 567-0047, Japan, Department of Chemistry, University of Wales, Bangor, Gwynedd LL57 3UW, U.K.

Received February 2, 2000

Monovalent cations ($M^+ = Na^+$, K^+, Rb^+, and NH_4^+) and 12-crown-4 were assembled to new supramolecular cation (SC^+) structures of the M^+(12-crown-4)$_n$ (n = 1 and 2), which were incorporated into the electrically conducting Ni(dmit)$_2$ salts (dmit = 2-thioxo-1,3-dithiole-4,5-dithiolate). The Na^+, K^+, and Rb^+ salts are isostructural with a stoichiometry of the M^+(12-crown-4)$_2$[Ni(dmit)$_2$]$_4$, while the NH_4^+ salt has a stoichiometry of NH_4^+(12-crown-4)[Ni(dmit)$_2$]$_3$(CH_3CN)$_2$. The electrical conductivities of the Na^+, K^+, Rb^+, and NH_4^+ salts at room temperature are 7.87, 4.46, 0.78, and 0.14 S cm^{-1}, respectively, with a semiconducting temperature dependence. The SC^+ structures of the Na^+, K^+, and Rb^+ salts have an ion-capturing sandwich-type cavity of M^+(12-crown-4)$_2$, in which the M^+ ion is coordinated by eight oxygen atoms of the two 12-crown-4 molecules. On the other hand, the NH_4^+ ion is coordinated by four oxygen atoms of the 12-crown-4 molecule. Judging from the M^+−O distances, thermal parameters of oxygen atoms, and vibration spectra, the thermal fluctuation of the Na^+(12-crown-4)$_2$ structure is larger than those of K^+(12-crown-4)$_2$ and Rb^+(12-crown-4)$_2$. The SC^+ unit with the larger alkali metal cation gave a stress to the Ni(dmit)$_2$ column, and the SC^+ structure changed the $\pi-\pi$ overlap mode and electrically conducting behavior.

Introduction

Novel supramolecular assemblies such as molecular chundles, molecular wires, molecular shuttles, and molecular trains have been attracting much attention from the viewpoints of its applications for molecular sensing, switching, and recognition devices.[1] Among a large number of molecules composing supramolecular systems, the "*crown ether*" is the first synthetic component that has the ability to recognize cations.[2] Various kind of cations are selectively complexed into the crown ether cavity, forming ion−macrocycle supramolecular cation units.[2]

The open-shell π radicals in a molecular conductor are assembled through the intermolecular $\pi-\pi$ interactions,[3] which also form interesting molecular systems regarded as supramolecular assemblies.[4] One category in the molecular conductors is the cation and/or anion radical salts, which have been providing a large number of organic metals and superconductors.[3] In these salts, closed-shell counteranions and/or anions are necessary to compensate for the charges in open-shell cations and anion species. We have been constructing novel molecular conductors by replacing the simple counterions to the supramolecular cation and/or anion systems within the crystals. The supramolecular cation (SC^+) structures are constructed through ion−crown ether complexation, which are incorporated into the Ni(dmit)$_2$ (dmit = 2-thioxo-1,3-dithiole-4,5-dithiolate) based molecular conductors having highly electrically conducting properties.[5−9] Through the design of the SC^+ structures within the molecular conductors, we can open up a new field of electron-conducting supramolecular systems. For example, we have recently reported the $Li^+_{0.6}$(15-crown-5)[Ni(dmit)$_2$]$_2$(H_2O)

* To whom correspondence should be addressed. Phone: +81-11-706-2884. Fax: +81-11-706-4972. E-mail: takuta@imd.es.hokudai.ac.jp.
† Research Institute for Electronic Science, Hokkaido University.
‡ Japan Science and Technology Corporation.
§ Gunma University.
|| Graduate School of Science, Hokkaido University.
⊥ Osaka University.
University of Wales.

(1) (a) Vögtle, F. *Supramolecular Chemistry, An Introduction*; John Wiley & Sons: Stuttgart, 1989. (b) Jörgensen, T.; Hansen, T.; Becher, J. *Chem. Rev.* **1994**, 41. (c) Lehn, J.-M. *Supramolecular Chemistry*; Anton, U., Ed.; VCH: Weinheim, 1995. (d) Nostrum, van, C. F. *Adv. Mater*. **1996**, *12*, 1027.
(2) (a) Weber, E.; Toner, J. L.; Goldberg, I.; Vögtle, F.; Laidler, D. A.; Stoddart, J. F.; Bartsch, R. A.; Liotta, C. L. *Crown ethers and analogs*; Patai, S., Rappoport, Z., Eds.; John Wiley & Sons: Stuttgart, 1989. (b) Gokel, G. *Crown Ethers & Cryptands*; Stoddart, J. F., Ed.; RSC, 1994.
(3) (a) Cowan, D. O. *New Aspects of Organic Chemistry*; Yoshida, Z., Shiba, T., Oshiro, Y., Eds.; Kodansha Ltd: Tokyo, 1989. (b) *Organic Conductors*; Farges, J.-P., Ed.; Marcel Dekker Inc: New York, 1994. (c) Ishiguro, T.; Yamaji, K.; Saito, G. *Organic Superconductors*; Fulde, P., Ed.; Springer-Verlag: New York, 1998.
(4) Akutagawa, T.; Hasegawa, T.; Nakamura, T. *Handbook of Advanced Electronic and Photonic Materials*; Nalwa, H. S., Ed.; Academic Press: San Diego, in press.
(5) Akutagawa, T.; Nakamura, T.; Inabe, T.; Underhill, A. E. *J. Mater. Chem*. **1996**, *7*, 135.
(6) Akutagawa, T.; Nakamura, T.; Inabe, T.; Underhill, A. E. *Synth. Met*. **1997**, *86*, 1961.
(7) Akutagawa, T.; Nakamura, T.; Inabe, T.; Underhill, A. E. *Thin Solid Films* **1998**, *331*, 264.
(8) Akutagawa, T.; Nezu, Y.; Hasegawa, T.; Nakamura, T.; Sugiura, K.; Sakata, Y.; Inabe, T.; Underhill, A. E. *Chem. Commun*. **1998**, 2599.
(9) Akutagawa, T.; Hasegawa, T.; Nakamura, T.; Sugiura, K.; Sakata, Y.; Inabe, T.; Underhill, A. E. *Synth. Met*. **1999**, *102*, 1747.

10.1021/ic000104a CCC: $19.00
Published on Web 05/24/2000

Chart 1

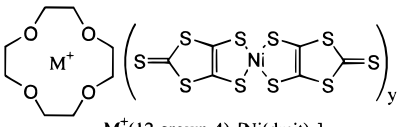

$M^+(12\text{-crown-4})_x[Ni(dmit)_2]_y$

1: $M^+ = Li^+$, x = 1.5, y = 3.5.
2: $M^+ = Na^+$, x = 2, y = 4.
3: $M^+ = K^+$, x = 2, y = 4.
4: $M^+ = Rb^+$, x = 2, y = 4.
5: $M^+ = NH_4^+$, x = 1, y = 3.

salt, which has a regular ion channel and an electrically conducting column simultaneously.[10]

This time we used 12-crown-4 as a host molecule to coordinate monovalent ions (M^+), and the resultant M^+(12-crown-4) structures were incorporated into electrically conducting $Ni(dmit)_2$ salts as new SC^+ structures. Our previous study of the $Li^+_2(12\text{-crown-4})_3[Ni(dmit)_2]_7(acetone)_2$ (**1**) salt revealed the formation of a novel dimeric pentacoordinated $Li^+_2(12\text{-crown-4})_3$ structure,[5] and preliminary structural analysis of the $NH_4^+(12\text{-crown-4})[Ni(dmit)_2]_3$ salt showed the formation of a pyramidal NH_4^+(12-corwn-4) structure within the crystals.[9] Since the coordination of 12-crown-4 in the SC^+ structures depends on the cation size, a systematic study involving changes in cation size from Li^+ to Na^+, K^+, Rb^+, and NH_4^+ should be necessary to obtain a general rule for designing the SC^+ structure in the electrically conducting salts. In this paper, we will describe the preparation, crystal structures, and electrically conducting behaviors of four kinds of new $M^+_x(12\text{-crown-4})[Ni(dmit)_2]_y$ salts ($M^+ = Na^+$, K^+, Rb^+, and NH_4^+) in addition to the Li^+ salt (Chart 1).[5] These $Ni(dmit)_2$ salts will be discussed in terms of the structural design of the SC^+ units within the $Ni(dmit)_2$-based molecular conductors.

Experimental Section

Crystal Preparation. The crystals were prepared using the standard electrocrystallization method. The single crystals of the salts **2**, **4**, and **5** were grown from the mixed solvent system (acetonitrile/acetone = 1:1), while salt **3** was obtained from the electrocrystallization in pure acetone. The stoichiometry of the crystals was determined by X-ray structural analysis. The Cs^+ salt was not obtained by the electrocrystallization method using $CsClO_4$ or CsI as a supporting electrolyte.

X-ray Crystal Structural Analysis. Crystal data were collected on Rigaku AFC-5R and -7R diffractometers with Mo Kα (λ = 0.710 73 Å) radiation at 296 K using a graphite monochromator. The crystal data of salt **2**, using the same crystal for the data collection at 296 K, were also collected at 190 K in order to reduce the disorders of the SC^+ structure. The structures were solved and refined using teXsan (Rigaku).[11] The structure refinements were performed by a full matrix least-squares method. Parameters were refined by the anisotropic temperature factors, and the hydrogen atoms were removed from the refinements. Large thermal parameters of the oxygen and carbon atoms of the 12-crown-4 molecule were observed in the structural analysis of salt **2** at 296 K. In this case, the positional disorders of the oxygen atoms were assumed at 190 K.

Transport Measurements. The temperature-dependent electrical conductivity was measured by the dc four-probe method along the long axis of the crystal, which is consistent with the stacking direction of $Ni(dmit)_2$. Electrical contacts of 10 μm gold wire to the crystals were made by gold paste (Tokuriki 8560).

(10) Nakamura, T.; Akutagawa, T.; Honda, K.; Underhill, A. E.; Coomber, A. T.; Friend, R. H. *Nature* **1998**, *394*, 159.
(11) *teXsan: Single crystal structure analysis software*, version 1.9, 1993.

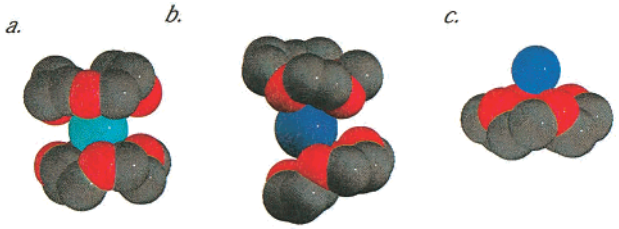

Figure 1. Supramolecular cation structures of M^+(12-crown-4) in the $Ni(dmit)_2$ salts: (a) $Na^+(12\text{-crown-4})_2$, (b) $K^+(12\text{-crown-4})_2$ and $Rb^+(12\text{-crown-4})_2$, and (c) NH_4^+(12-crown-4) units viewed parallel to the 12-crown-4 plane.

Calculation of Transfer Integrals. The transfer integrals (t) were calculated within the tight-binding approximation using the extended Hückel molecular orbital calculation. The LUMO of the $Ni(dmit)_2$ molecule was used as the basis function.[12] The semiempirical parameters for Slater-type atomic orbitals were used.[12] The t values between each pair of molecules is assumed to be proportional to the overlap integral (s), $t = Es$, where E is −10.0 eV.

Results and Discussion

Crystal Structures. Table 1 summarizes the crystal data of the salts **1**, $Na^+(12\text{-crown-4})_2[Ni(dmit)_2]_4$ (**2**), $K^+(12\text{-crown-4})_2[Ni(dmit)_2]_4$ (**3**), $Rb^+(12\text{-crown-4})_2[Ni(dmit)_2]_4$ (**4**), and $NH_4^+(12\text{-crown-4})[Ni(dmit)_2]_3(CH_3CN)_2$ (**5**). The salts **2**−**4** have the same stoichiometry. Figure 1 shows the change in SC^+ structure by changing the ion size from Na^+ to K^+, Rb^+, and NH_4^+. The SC^+ structures of salts **2**−**4** are quite significantly different from the $Li^+_2(12\text{-crown-4})_3$ unit found in salt **1**.[5] Salts **3** and **4** have a higher crystal symmetry ($P2_12_12$) than that of salt **2** ($P2_1/c$); however, these three salts are isostructural to each other. The increase in the ionic radius from Li^+ (0.68 Å) to Na^+ (0.97 Å), K^+ (1.33 Å), and Rb^+ (1.52 Å) changed the SC^+ structure from dimeric pentacoordination to sandwich-type ($M^+ = Na^+$, K^+, and Rb^+). On the other hand, salt **5** has a different crystal structure and the SC^+ unit is the pyramidal tetracoordinated NH_4^+(12-crown-4). The structural diversity of the SC^+ units depends on the character and size of incorporated cations. The details of structural parameters of the $Ni(dmit)_2$ layers and the SC^+ units are summarized in parts a and b of Table 2, respectively, which will be discussed in the following sections.

1. $M^+(12\text{-crown-4})_2[Ni(dmit)_2]_4$ Salts ($M^+ = Na^+$, K^+, and Rb^+). Two kinds of the $Ni(dmit)_2$, **A** and **B**, and one M^+(12-crown-4) unit of salts **2**−**4** make up the crystallographically asymmetric unit. Parts a and b of Figure 2 show the unit cell of the salt **2** viewed along the a and the b axes, respectively. The $Ni(dmit)_2$ molecules form a nonuniform stack along the a axis in which the **A**−**B** dimer is a fundamental unit (Figure 2b). The mean interplanar distance of the **A**−**B** dimer (d_1) found in salt **2** is ca. 0.2 Å shorter than that of the interdimer **A**−**B′** (d_2). The intradimer d_1 distances of salts **3** and **4** were also ca. 0.3 and 0.5 Å shorter than those of the interdimer, respectively.

The dimerization is further supported by the calculation of the transfer integrals ($t \times 10^{-2}$ eV). Figure 2c shows the transfer integrals of the electrically conducting $Ni(dmit)_2$ layer viewed along the long axis of the $Ni(dmit)_2$ molecule. The intradimer interaction ($t_1 = -14.28$) of salt **2** is twice that of the interdimer ($t_2 = 7.08$) at 296 K. Lowering of the temperature to 190 K

(12) (a) Mori, T.; Kobayashi, A.; Sasaki, Y.; Kobayashi, H.; Saito, G.; Inokuchi, H. *Bull. Chem. Soc. Jpn.* **1984**, *57*, 627. (b) Summerville, R. H.; Hoffmann, R. J. *J. Am. Chem. Soc.* **1976**, *98*, 7240. (c) Berlinsky, A. J.; Carolan, J. F.; Weiler, L. *Solid State Commun.* **1974**, *15*, 795.

Table 1. Crystal Data, Data Collection, and Reduction Parameter of the M^+_x(12-crown-4)[Ni(dmit)$_2$]$_y$ Salts

	1[a]	**2**	**2′**	**3**	**4**	**5**
chemical formula	$C_{72}H_{60}O_{14}S_{70}Ni_7Li_2$	$C_{40}H_{32}O_8S_{40}Ni_4Na$	$C_{40}H_{32}O_8S_{40}Ni_4Na$	$C_{40}H_{32}O_8S_{40}Ni_4K$	$C_{40}H_{32}O_8S_{40}Ni_4Rb$	$C_{30}H_{26}NO_4S_{30}Ni_3$
fw	3818.12	2180.88	2180.88	2196.99	2243.36	1602.44
cryst syst	triclinic	monoclinic	monoclinic	orthorhombic	orthorhombic	monoclinic
space group	$P\bar{1}$ (No. 2)	$P2_1/c$ (No. 14)	$P2_1/c$ (No. 14)	$P2_12_12$ (No. 18)	$P2_12_12$ (No. 18)	$P2/n$ (No. 13)
crystal size, mm^3	0.5 × 0.3 × 0.1	0.6 × 0.2 × 0.1	0.6 × 0.2 × 0.1	1.2 × 0.2 × 0.05	0.6 × 0.2 × 0.1	0.5 × 0.1 × 0.1
a, Å	9.075(4)	8.055(6)	8.068(6)	8.036(3)	7.939(6)	8.793(7)
b, Å	18.370(5)	11.23(1)	11.084(4)	11.420(2)	11.548(4)	7.537(6)
c, Å	20.677(5)	41.97(1)	41.711(5)	41.398(6)	41.604(7)	43.701(5)
α, deg	91.38(2)					
β, deg	93.83(3)	91.63(8)	92.53(4)			94.19(3)
γ, deg	103.86(3)			8.036(3)		
V, Å^3	3336(2)	3794(4)	3726(2)	3799(1)	3814(2)	2888(2)
Z	1	2	2	2	2	2
D_{calc}, g cm^{-1}	1.904	1.909	1.944	1.920	1.953	1.842
temp, K	296	296	190	296	296	296
μ, cm^{-1}	12.04	21.69	21.69	21.77	27.46	20.89
R[b]	0.076	0.075	0.080	0.043	0.079	0.052
R_w[b]	0.075	0.083	0.080	0.039	0.045	0.057

[a] Crystal data were cited from ref 5. [b] $R = \sum||F_o| - |F_c||/\sum|F_o|$ and $R_w = (\sum w(|F_o| - |F_c|)^2/\Sigma(wF_o^2)^{1/2}$.

Table 2

(a) Mean Interplanar Distances (d_1 and d_2, Å) and Intracolumn (t_{intra}) and Intercolumn Transfer Integrals ($t_{Inter} \times 10^{-2}$ eV) within the Ni(dmit)$_2$ Layer[a]

	2	**2′** [b]	**3**	**4**	**5**
d_1	3.454	3.430	3.269	3.291	3.374
d_2	3.668	3.604	3.666	3.794	3.502
intracolumn					
t_1	−14.28	−15.25	−14.33	−12.58	−19.06
t_2	7.08	5.13	1.27	2.81	−3.26
intercolumn					
t_3	0.26	0.21	0.15	−0.54	0.24
t_4	0.04	0.12	−1.49	−0.82	−1.46
t_5	−1.34	−1.41	0.53	0.15	0.36
t_6	0	0.29	−0.51	−1.06	0.24

(b) Interatomic M^+−O Distances (Å), Average M^+−O_{AV} Distance (Å), van der Waals Distance M^+−O_{vdw} (Å), Average Isotropic Thermal Parameter of the Oxygen Atom (B_{eq}), Energies of Asymmetric COC Stretching Mode (ν^a_{COC}, cm^{-1}), and Displaced Distances of the M^+ Ions from the Mean Oxygen Plane of the 12-Crown-4 (d_M, Å), within the SC^+ Units

	2	**2′** [b]	**3**	**4**	**5**
M^+−O					
M^+−O1, O5	2.62(2)	3.38(2), 2.35(2)	2.917(10)	3.05(2)	2.92(1)
M^+−O2, O6	2.79(3)	3.42(2), 2.59(2)	2.871(9)	3.00(2)	2.85(1)
M^+−O3	2.76(2)	2.77(2)	2.744(8)	2.92(1)	
M^+−O4, O7	2.84(3)	3.47(2), 2.20(2)	2.883(9)	3.05(2)	
M^+−O_{av}	2.75	2.48	2.85	3.01	2.89
M^+−O_{vdw}	2.47	2.47	2.85	3.00	2.87
B_{eq}	16.1	6.1	8.6	9.1	7.2
ν^{a1}_{COC}	1023	1022	1024	1024	1023
ν^{a2}_{COC}	1094	1094	1100	1100	1100
ν^{a3}_{COC}	1134	1134[c]	1134	1134	1134
d_M	1.80	1.80	2.03	2.25	2.05

[a] Mean interplanar distances were determined by 17 atoms of the Ni(dmit)$_2$ molecules. [b] Based on the structural analysis at 190 K. [c] Determied at 100 K.

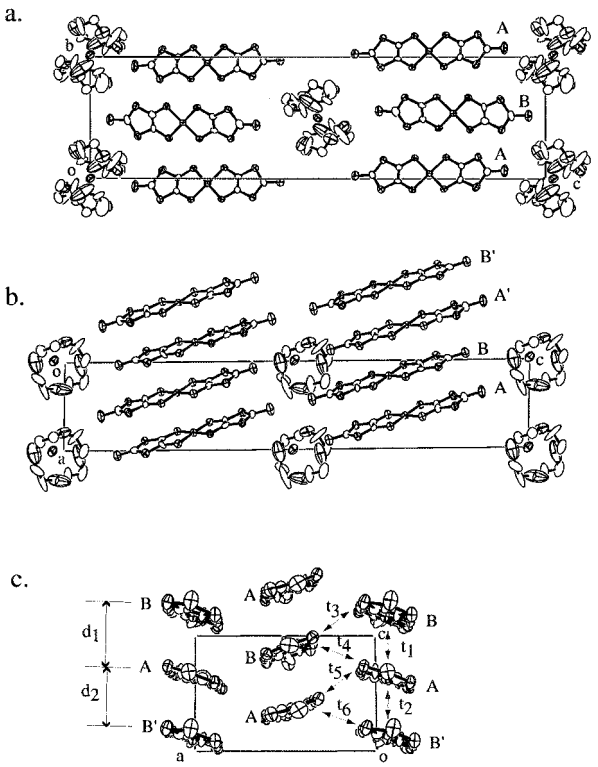

Figure 2. Crystal structure of the Na^+(12-crown-4)$_2$[Ni(dmit)$_2$]$_4$ salt viewed along the *a* axis (a) and along the *b* axis (b). (c) Electrically conducting Ni(dmit)$_2$ layer within the *ac* plane viewed along the long axis of the Ni(dmit)$_2$ molecule. The transfer integrals (t_1−t_6) and mean interplanar distances (d_1 and d_2) indicated in the figure are summarized in Table 2a.

increases the degree of dimerization ($t_1 = -15.25$ and $t_2 = 5.13$), although the difference in the interplanar distances between intra- and interdimer is reduced at lower temperature. The strong dimerization is also observed in salts **3** ($t_1 = -14.33$ and $t_2 = 1.27$) and **4** ($t_1 = -12.58$ and $t_2 = 2.81$).

Each Ni(dmit)$_2$ dimer of salt **2** is connected by the side by side S−S interactions along the $2a - c$ (t_3 and t_5) and the $2a + c$ (t_4 and t_6) directions. The magnitude of the transverse transfer integrals ($t_3 - t_6 = 0.26 - 1.34$) is not effective for increasing the intercolumn interactions and the electrical dimensionality of the Ni(dmit)$_2$ layer (Table 2a). The interaction between **A** molecules along the $2a - c$ direction ($t_5 = -1.34$) is the most effective, the magnitude of which is, however, 5 times smaller than that of the intracolumn ($t_2 = 5.13$). In the cases of salts **3** and **4**, the effective transverse interactions are elongated along the $2a + c$ direction ($t_4 = -1.49$ of salt **3** and $t_6 = -1.06$ of salt **4**). These are also too small to increase the transverse interactions and electrical dimensionality of the Ni(dmit)$_2$ layer.

2. SC^+ Structures of M^+(12-crown-4)$_2$ Units. The Na^+, K^+, and Rb^+ ions are coordinated by eight oxygen atoms of two 12-crown-4 molecules, forming sandwich-type M^+(12-crown-4)$_2$ structures (parts a and b of Figure 1). Each M^+(12-crown-

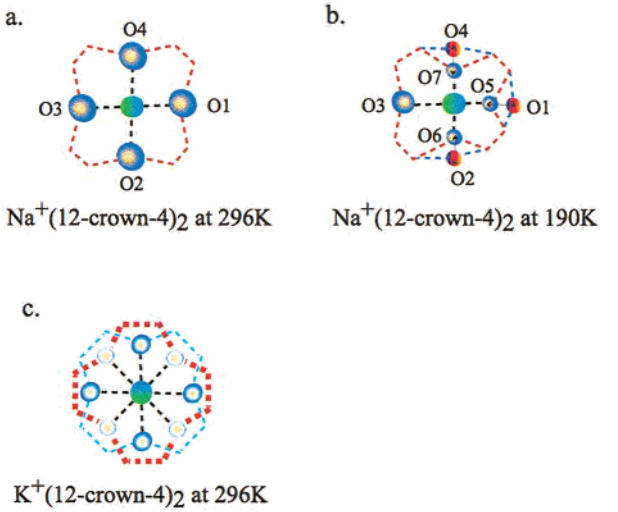

Figure 3. Schematic oxygen arrangements of the $M^+(12\text{-crown-4})_2$ units: (a) $Na^+(12\text{-crown-4})_2$ at 296 K; (b) $Na^+(12\text{-crown-4})_2$ at 190 K; (c) $K^+(12\text{-crown-4})_2$ at 296 K.

4)$_2$ unit is located at the space between the Ni(dmit)$_2$ layers, and the molecular plane of the 12-crown-4 is normal to the Ni(dmit)$_2$ plane. The $M^+(12\text{-crown-4})_2$ units are arranged along the *b* axis without intermolecular interaction with the other SC^+ units and with the Ni(dmit)$_2$ layers. As a result, the SC^+ units and the electrically conducting Ni(dmit)$_2$ layers are isolated from each other.

Although the formation of the sandwiched cavities has been reported in the $Li^+(12\text{-crown-4})_2$,[13] $Na^+(12\text{-crown-4})_2$,[14] $K^+(12\text{-crown-4})_2$[dichlorobis(pentacarbonylchromium)],[15] $Ag^+(12\text{-crown-4})_2PF_6$,[16] $Fe^{2+}(12\text{-crown-4})_2(PF_6^-)_2$,[17] and $Mn^{2+}(12\text{-crown-4})_2(Br_3^-)_2$,[18] the $Rb^+(12\text{-crown-4})_2$ structure has not been reported so far to our knowledge. Since the ionic radii of Na^+, K^+, and Rb^+ are larger than the cavity radius of the 12-crown-4 molecule (0.6−0.75 Å), the coordinated structure of sandwich-type $M^+(12\text{-crown-4})_2$ in salts **2**−**4** is most reasonable. The coordination properties found in the above simple salts were conserved for SC^+ units in the Ni(dmit)$_2$-based molecular conductors. One exception is the $Li^+{}_2(12\text{-crown-4})_3$ found in salt **1**.[5] The sandwich-type $Li^+(12\text{-crown-4})_2$ may be too small to hold the same packing arrangements of the Ni(dmit)$_2$ found in salts **2**−**4**. The conformational freedom of 12-crown-4 molecules is influenced by the strength of coordination from the oxygen atoms of 12-crown-4 molecule to M^+. The thermal parameters of oxygen atoms and M^+−O distances are good indicators for the thermal fluctuation of the $M^+(12\text{-crown-4})_2$ units (Table 2b). The $Na^+(12\text{-crown-4})_2$ structure largely fluctuates at 296 K, which was confirmed by the large magnitude of average isotropic thermal parameter of oxygen atoms (B_{eq} = 16.1). Since it was impossible to obtain a reasonable coordinated structure with small B_{eq} values, assuming several disordered arrangements, we considered that the fluctuation is intrinsic (Figure 3a). The average Na^+−O distance of 2.75 Å is ca. 0.2 Å longer than the van der Waals (v.d.W.) contact.[19] The weak Na^+−O coordination property should be the reason for the conformational fluctuations of the $Na^+(12\text{-crown-4})_2$ structure and large thermal parameters.

The magnitude of the thermal fluctuation in the $Na^+(12\text{-crown-4})_2$ structure was largely reduced at 190 K, and we could introduce the conformational disorder in the structural determination. Three pairs of disordered arrangements in oxygen atoms (O5−O1, O6−O2, and O7−O4) were assumed with occupancy factors of 0.5 (Figure 3b). Four kinds of effective Na^+−O contacts (Na^+−O5, Na^+−O6, Na^+−O3, and Na^+−O7) are found within the range of v.d.W. contacts;[19] however, the other Na^+−O contacts are too long to coordinate the Na^+ ion into the cavity. The average Na^+−O distance of 2.48 Å is derived from the former effective Na^+−O distances, and the B_{eq} value (6.1) at 190 K is ca. 3 times smaller than that found in 296 K. The thermally fluctuating 12-crown-4 structure at 296 K gradually fixed in disordered conformations with coordinations to Na^+ from the O3, O5, O6, and O7 oxygen atoms. However, the O1, O2, and O4 atoms exist in an environment close to that of free 12-crown-4 molecule.

The structure of $K^+(12\text{-crown-4})_2$ in salt **3** at 296 K is shown in Figure 3c. The $K^+(12\text{-crown-4})_2$ and $Rb^+(12\text{-crown-4})_2$ units are isostructural; however, the angle between two 12-crown-4 planes of the $Rb^+(12\text{-crown-4})_2$ (35.1°) defined by four oxygen atoms is larger than that of $K^+(12\text{-crown-4})_2$ (29.5°). Since the disorders of the 12-crown-4 molecules are not observed and the B_{eq} values found in salts **3** (B_{eq} = 8.6) and **4** (B_{eq} = 9.1) are in reasonable range, the SC^+ structures of salts **3** and **4** are already fixed at 296 K. In addition, the average K^+−O and Rb^+−O distances are almost the same as those of the v.d.W. contacts.[19] An increase in the ion size from Na^+ to K^+ or Rb^+ reduced the structural fluctuations of the $M^+(12\text{-crown-4})_2$ units through the increase in the M^+−O interactions.

The increase in the ion size from Na^+ to K^+ and Rb^+ decreases the *a*-axis length (a = 8.055(6), 8.036(3), and 7.939(6) Å) and increases the *b*-axis length (b = 11.23(1), 11.420(2), and 11.548(4) Å). The Ni(dmit)$_2$ stacks are compressed along the stacking axis, while the magnitudes of side by side interactions are reduced with an increase in the ion size. The change in ion size of the $M^+(12\text{-crown-4})_2$ units also influences the electronic structure of the Ni(dmit)$_2$ stack in addition to the structural fluctuations in the SC^+ units, which perturbs the electrically conducting properties of these salts.

3. $NH_4^+(12\text{-crown-4})[Ni(dmit)_2]_3(CH_3CN)_2$ Salt. A half unit of the Ni(dmit)$_2$ **A**, one Ni(dmit)$_2$ **B**, and a half unit of the NH_4^+-(12-crown-4) are crystallographically asymmetric units. Figure 4 shows the unit cell of salt **5** viewed along the $-a + b$ axis. Two kinds of Ni(dmit)$_2$ column, columns a and b, are elongated along the $a + b$ and $-a + b$ axes, respectively, and these are orthogonal to each other. The fundamental unit of the Ni(dmit)$_2$ column is the **B**−**A**−**B′** trimer, and the two-dimensional layer structure within the *ab* plane is constructed through the short interatomic S−S contacts between the Ni(dmit)$_2$ columns. The **A**−**B** mean interplanar distance is ca. 0.13 Å shorter than the **B**−**B′** pairs. Figure 4b shows the transfer integrals of the electrically conducting Ni(dmit)$_2$ layer (column a) viewed along the long axis of the Ni(dmit)$_2$. The intratrimer interaction (t_1 = −19.02) is ca. 6 times larger than that of the intertrimer (t_2 = −3.26), indicating a strong trimerization of the **B**−**A**−**B′** unit. The side by side transverse interactions in column a are elongated along the $2a + b$ (t_3 and t_5) and the *b* axes (t_4 and t_6),

(13) Hope, H.; Olmstead, M. M.; Power, P. P.; Xu, X. *J. Am. Chem. Soc.* **1984**, *106*, 819.
(14) Chen, H.; Jutzi, P.; Leffers, W.; Olmstead, M. M.; Power, P. P. *Organometallics* **1991**, *10*, 1282.
(15) Schiemenz, B.; Antelmann, B.; Huttner, G.; Zsolnai, L. *Z. Anorg. Allg. Chem.* **1994**, *620*, 1760.
(16) Hughes, B. B.; Haltiwanger, R. C.; Pierpont, C. G.; Hampton, M.; Blackmer, G. L. *Inorg. Chem.* **1980**, *19*, 1801.
(17) Jones, P. G.; Gries, T.; Grutzmacher, H.; Roesky, H. W.; Schimkowiak, J.; Sheldrick, G. M. *Angew. Chem., Int. Ed. Engl.* **1984**, *23*, 376.
(18) Meier, K.; Rihs, G. *Angew. Chem., Int. Ed. Engl.* **1985**, *24*, 858.
(19) Bondi, A. *J. Phys. Chem.* **1964**, *68*, 441.

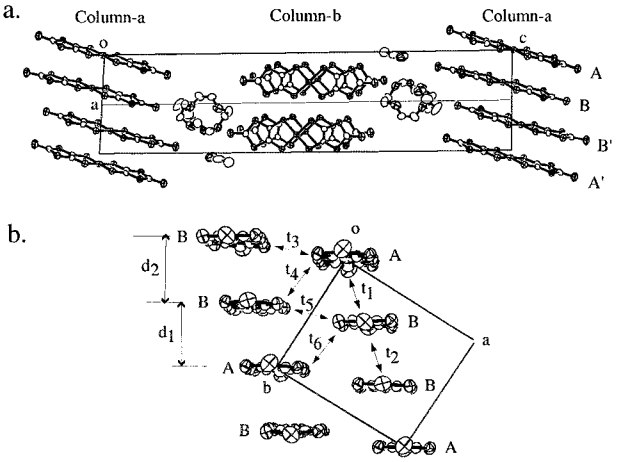

Figure 4. Crystal structure of the NH_4^+(12-crown-4)$[Ni(dmit)_2]_3(CH_3CN)_2$ salt: (a) viewed along the $-a + b$ axis; (b) electrically conducting layer (column a) viewed along the long axis of the $Ni(dmit)_2$ molecules. The transfer integrals (t_1-t_6) and mean interplanar distances (d_1 and d_2) indicated in the figure are sumarized in Table 2a.

while those in column b are along the $a + 2b$ and the a axes, respectively. The t_4 interaction (-1.46) along the b axis is the most effective among the four transverse ones. However, the magnitude of the transverse interaction is not effective enough to increase the electrical dimensionality of the $Ni(dmit)_2$ layer.

4. SC^+ Structures of NH_4^+(12-crown-4) Unit. The SC^+ structure of salt **5** is composed of pyramidal coordination of the NH_4^+ by four oxygen atoms of the 12-crown-4 molecule (Figure 1c). The SC^+ structure of the NH_4^+(12-crown-4) is fixed at one conformation without disorders. The SC^+ structures are located at the space between the $Ni(dmit)_2$ layers and stacked along the b axis. Although the ionic radius of NH_4^+ ion is almost the same as that of K^+ or Rb^+, only the pyramidal structure of NH_4^+(12-crown-4) was obtained.

A driving force for the formation of the NH_4^+(12-crown-4) pyramidal structure may be the hydrogen-bonding ability of the NH_4^+ ion to the oxygen atoms of the 12-crown-4 molecule.[20] The average N1−O distance of 2.89 Å is about the same as the standard hydrogen-bonding distance of NH_4^+−O (2.87 Å).[20] The NH_4^+ ion is displaced 2.1 Å from the mean oxygen plane of the 12-crown-4 molecule. The B_{eq} value of the oxygen atoms (7.2) is found in a reasonable range, which indicates the less fluctuating structure of the NH_4^+(12-crown-4) unit than that of the Na^+(12-crown-4)$_2$ in salt **2** at 296 K.

The common structural feature of the M^+(12-crown-4) SC^+ system is the outside arrangements of the M^+ ions against the 12-crown-4 cavity due to the smaller cavity radius compared to the size of the ions used in this study. The sandwich-type $M^+(12\text{-crown-4})_2$ structure is typically observed in the 12-crown-4 coordinated Li^+, Na^+, and K^+ salts.[13−15] However, a similar sandwich-type structure of $NH_4^+(12\text{-crown-4})_2$ has not been reported. The increase in SC^+ size from the pyramidal NH_4^+(12-crown-4) to the sandwich-type $Na^+(12\text{-crown-4})_2$, K^+-(12-crown-4)$_2$, and $Rb^+(12\text{-crown-4})_2$ changes the $M^+/Ni(dmit)_2$ ratio from the 1:3 to 1:4. The 1:4 stoichiometry has been also reported in a salt with a large SC^+ system, Na^+(*cis*,*anti*,*cis*-dicyclohexyl-18-crown-6)$[Ni(dmit)_2]_4$.[21] The $M^+/Ni(dmit)_2$ stoichiometry is sensitive to the size of cations. For example, the

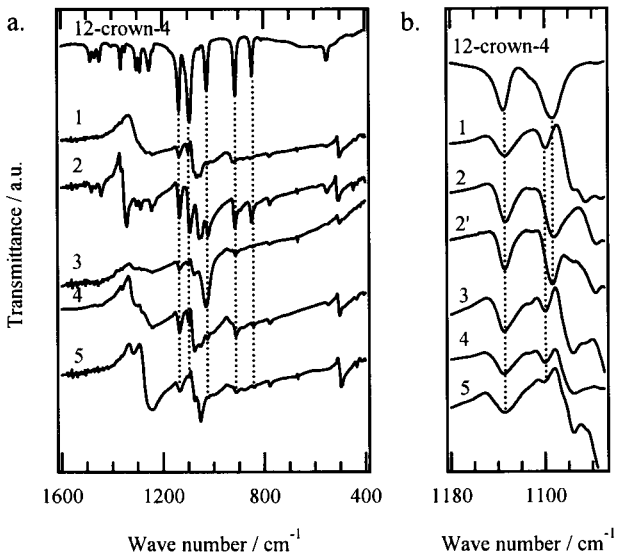

Figure 5. Vibrational spectra of the salts **1**−**5** and free 12-crown-4 molecule in the energy regions of (a) 400−1600 and (b) 1050−1180 cm^{-1}.

1:3 stoichiometry of the $(Ph_3P)[Ni(dmit)_2]_3$ salt[22] changed to 1:4 in $(Ph_3As)[Ni(dmit)_2]_4$.[23] The stacking arrangements of the $Ni(dmit)_2$ column are quite significantly influenced by the $SC^+/Ni(dmit)_2$ stoichiometry or the charge on $Ni(dmit)_2$. The 1:3 salts typically have trimer stacks of the $Ni(dmit)_2$, while the 1:4 salts have dimer stacks. Thus, the design of the SC^+ structures in both size and shape is important for controlling the electrically conducting properties of the $Ni(dmit)_2$ salts.

Vibrational Spectra. The dynamics of M^+(12-crown-4) units incorporated in $Ni(dmit)_2$ salts were further examined by analyzing the vibrational spectra. Figure 5a shows the IR spectra of salts **1**−**5** and the free 12-crown-4 molecule in the energy region 400−1600 cm^{-1}. Enlarged spectra in the energy region 1050−1180 cm^{-1} are shown in Figure 5b.

The free 12-crown-4 molecule has some characteristic IR-active bands that are assigned to the COC asymmetric stretching modes ($\nu^{a1}_{COC} = 1026$, $\nu^{a2}_{COC} = 1094$, and $\nu^{a3}_{COC} = 1135$ cm^{-1}) and the COC symmetric vibration (ν^{s}_{COC} = 845 and 915 cm^{-1}).[24] The vibrational spectra of the salts **1**−**5** clearly show that the peaks correspond to the ν^{a}_{COC} and ν^{s}_{COC} modes of the 12-crown-4 molecule (see also Table 2b). The strong M^+−O interactions within the SC^+ structures cause the shift of the ν^{a2}_{COC} mode.[24] However, the magnitude of the energy shift is small and depends on the ring size of the crown ethers. A blue shift of 6 cm^{-1} has been reported for the Mn^{2+}(12-crown-4)-Cl^-_2 salt.[24] The ν^{a3}_{COC} modes of salts **1**−**5** (1134 cm^{-1}) appear at the same position as the free 12-crown-4 molecule, while the ν^{a2}_{COC} mode in salts **1** and **3**−**5** (1100 cm^{-1}) shows a slight blue shift of about 6 cm^{-1}. The latter mode in salt **2** (1094 cm^{-1}) is observed at the same position as that of the free 12-crown-4 molecule, and the low-temperature IR measurements at 100 K also showed no spectral change in the ν^{a}_{COC} mode. The COC bonds of the $Na^+(12\text{-crown-4})_2$ are largely fluctuating in the crystal, and the environment of the 12-crown-4 molecule should be close to that of the free 12-crown-4 molecule, which is consistent with the results of the X-ray structural analysis.

(20) Jeffrey, G. A. *An Introduction to Hydrogen Bonding*; Oxford University Press Inc: New York, 1997. (b) Hamilton, W. C.; Ibers, J. A. *Hydrogen Bonding in Solids*; Benjamin: New York, 1968.
(21) Robertson, N.; Akutagawa, T.; Nakamura, T.; Roehrs, S.; Underhill, A. E. *J. Mater. Chem.* **1999**, *9*, 1233.
(22) Nakamura, T.; Underhill, A. E.; Coomber, A. T.; Friend, R. H.; Tajima, H.; Kobayashi, A.; Kobayashi, H. *Inorg. Chem.* **1995**, *34*, 870.
(23) Valade, L.; Legros, J.-P.; Cassoux, P.; Kubel, F. *Mol. Cryst. Liq. Cryst.* **1986**, *140*, 335.
(24) Li, H.; Jiang, T.; Butler, I. S. *J. Raman Spectrosc.* **1989**, *20*, 560.

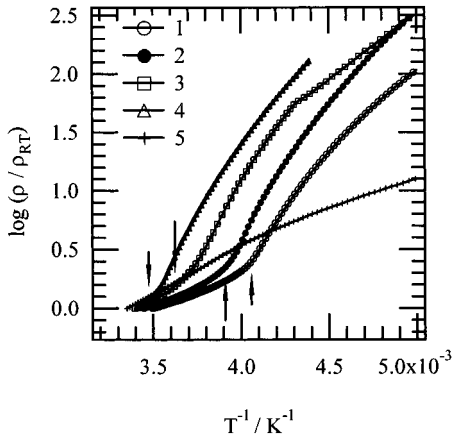

Figure 6. Logarithmic resistivity normalized at room temperature (log-(ρ/ρ_{RT})) vs inverse of temperature (T^{-1}) plots of salts **1** (○), **2** (●), **3** (□), **4** (△), and **5** (+). The arrows indicate the transition temperature from the α phase to the β phase.

Table 3. Electrical Conductivities at Room Temperature (σ_{RT}, S cm^{-1}), Semiconductor−Semiconductor Transition Temperatures (T_{ss}, K), and Activation Energies ($E_a(\alpha)$ and $E_a(\beta)$, eV) of the Salts **1**−**5**

salt	σ_{RT},[a] S cm^{-1}	T_{SS}, K	$E_a(\alpha)$[b], eV	$E_a(\beta)$[b], eV
1	30.0	230	0.10	0.17
2	7.87	255	0.14	0.49
3	4.46	270	0.17	0.35
4	0.78	280	0.30	0.45
5	0.14		0.14	

[a] Measured by the standard four-probe dc method. [b] The activation energies $E_a(\alpha)$ and $E_a(\beta)$ correspond to higher (α phase) and lower (β phase) temperature regions than transition temperatures T_{ss}.

Electrical Conductivity. Table 3 summarizes the electrical properties of salts **1**−**5**. The semiconducting temperature-dependent behaviors are observed in all salts. The σ_{RT} values of salts **1**−**5** are 30.0, 7.87, 4.46, 0.78, and 0.14 S cm^{-1}, respectively, and the values decrease according to the ion size ($Na^+ > K^+ > Rb^+$) when we compare isostructural salts **2**−**4**. Figure 6 shows the logarithmic resistivity normalized at room temperature (log(ρ/ρ_{RT})) vs the inverse of the temperature (T^{-1}) plots. Salts **1**−**4** show nonlinear behavior with two semiconducting phases at the higher (α-phase) and lower temperature regions (β-phase). The transition points between the α and β phases are indicated by arrows. The transition temperatures (T_{ss}) from the α to the β phases of salts **1**−**4** are 230, 255, 270, and 280 K, respectively. The magnitudes of the T_{ss} values of the isostructural salts are consistent with the sequence of the cation size ($Na^+ < K^+ < Rb^+$). The increase in the ion size from Na^+ to K^+ to Rb^+ stabilizes the low-temperature β phases. On the other hand, almost linear temperature-dependent behavior is observed for salt **5** with an activation energy of 0.14 eV. The activation energies $E_a(\alpha)$ of salts **1**, **2**, **3**, and **4** in the α phase are 0.10, 0.14, 0.17, and 0.30 eV, respectively. The magnitude of the $E_a(\alpha)$ values are also correlated to the ion size ($Na^+ < K^+ < Rb^+$). The activation energies $E_a(\beta)$ of salts **1**, **2**, **3**, and **4** in the β phase are 0.17, 0.49, 0.35, and 0.45 eV, respectively, and the values are larger than the $E_a(\alpha)$ of each salt. The stacking manner of the Ni(dmit)$_2$ columns as well as the SC^+ structures of salts **1** and **5** is quite significantly different from that of salts **2**−**4**. We will discuss the relationship between the conductivity and the ion size for the isostructural series of salts **2**−**4**.

The conducting π electrons on the Ni(dmit)$_2$ column should be influenced by the SC^+ structures in the solid. There are two interactions between the SC^+ and Ni(dmit)$_2$ lattice. One is the change in the magnitude of the lattice distortions in the Ni(dmit)$_2$ column by changing the SC^+ size, which should be the dominant factor for influencing the electrical conduction. The other is the change in the magnitude of the conformational fluctuation in the SC^+ system; this may be associated with the order−disorder transition. The strong dimerized structure of the Ni(dmit)$_2$ column was observed in salts **2**−**4**. However, the magnitudes of interdimer interactions in salts **3** ($t_2 = 1.27$) and **4** ($t_2 = 2.81$) are quite significantly smaller than that of salt **2** ($t_2 = 7.08$). The increase in ion size from Na^+ to K^+ or Rb^+ enhances the interdimer lattice distortion while holding the same stoichiometry, which decreases the electrical conductivity. The fluctuation in the SC^+ structure seems to have a small influence on the electrically conducting behavior of the Ni(dmit)$_2$ lattice even for the Na^+ salt. The stoichiometry of simple M^+[Ni(dmit)$_2$]$_y$ salts largely depends on the cation size, Na^+[Ni(dmit)$_2$]$_2$, K^+[Ni(dmit)$_2$]$_{2.5}$, and Rb^+[Ni(dmit)$_2$]$_{2.78}$,[25] and the cation size largely influences the stacking manner of the Ni(dmit)$_2$ columns. On the other hand, the 12-crown-4 based SC^+ structures can hold the same M^+(12-crown-4)$_2$[Ni(dmit)$_2$]$_4$ stoichiometry and Ni(dmit)$_2$ dimer structure in the Na^+, K^+, and Rb^+ salts. Since the 12-crown-4 has structural flexibility and some stable conformations, the volume change from Na^+ to K^+ and Rb^+ is relaxed by the conformational change of the 12-crown-4 molecules. The larger ion size decreases the structural flexibility of the crown ether and fixes the conformation of the 12-crown-4 in the crystal. The M^+−Ni distances between the M^+ and Ni(dmit)$_2$ **A** (or Ni(dmit)$_2$ **B**) for salts **2**, **2′**, **3**, and **4** decrease from 12.55 (12.17), 12.52 (11.07), 12.42 (9.90), and 12.12 Å (9.90 Å), respectively. The large M^+(12-crown-4)$_2$ unit gives stress to the Ni(dmit)$_2$ column, which distorts the $\pi-\pi$ overlap in the stack and reduces the electrical conductivity. The fine-tuning of electrically conducting behavior may be possible by utilizing the structures of SC^+ units.

Summary

New supramolecular cation (SC^+) structures based on 12-crown-4 were incorporated into the electrically conducting Ni(dmit)$_2$ salts. The SC^+ structures are composed of the M^+ ions ($M^+ = Li^+$, Na^+, K^+, Rb^+, and NH_4^+) coordinated by the 12-crown-4 molecules, which give a novel Rb^+(12-crown-4)$_2$ structure. The M^+(12-crown-4)$_2$[Ni(dmit)$_2$]$_4$ salts ($M^+ = Na^+$, K^+, and Rb^+) have the sandwich-type M^+(12-crown-4)$_2$ SC^+ structure, whereas a pyramidal NH_4^+(12-crown-4) structure was observed in the NH_4^+(12-crown-4)[Ni(dmit)$_2$]$_3$(CH$_3$CN)$_2$ salt. The 12-crown-4 molecule in the Na^+ salt has motional freedom as free 12-crown-4 at room temperature, and a disordered arrangement of the Na^+(12-crown-4) structure was found even at 190 K. On the other hand, the 12-crown-4 molecule in the Li^+, K^+, Rb^+, and NH_4^+ salts are already fixed in one conformation at room temperature.

Segregated nonuniform stacks of the Ni(dmit)$_2$ were found in all salts. The large monovalent cations (K^+ and Rb^+) form asymmetric sandwich-type M^+(12-crown-4)$_2$ SC^+ structures and increase the size of SC^+ cations. The interdimer interaction found in the Ni(dmit)$_2$ column was reduced by changing the Na^+ ion to the K^+ and Rb^+ ions, which influences the conducting behavior of the Ni(dmit)$_2$ column. The structure of the SC^+ unit was closely related to the stacking manner of the electrically conducting Ni(dmit)$_2$ columns. Two kinds of semiconducting phases (α and β phases) were observed in the

(25) Cassoux, P.; Valade, L.; Kobayashi, H.; Kobayashi, A.; Clark, R. A.; Underhill, A. E. *Coord. Chem. Rev.* **1991**, *110*, 115.

Li^+, Na^+, K^+, and Rb^+ salts. The room-temperature conductivity decreased according to the cation size (Na^+, K^+, and Rb^+ salts), and the transition temperatures between the α and β phases and the activation energy of α phases were also correlated to the cation size in the isostructural salts. The electrically conducting behavior of these salts were finely tuned utilizing the SC^+ structure.

Acknowledgment. This work was partly supported by a Grant-in-Aid for Science Research from the Ministry of Education, Science, Sports, and Culture of Japan and by the Proposal-Based New Industry Creative Type Technology R&D Promotion Program from the New Energy and Industrial Technology Development Organization (NEDO) in Japan.

Supporting Information Available: Five X-ray crystallographic files in CIF format. This material is available free of charge via the Internet at http://pubs.acs.org.

IC000104A